Mechanism of Accumulation of ^{99m}Tc-Sulesomab in Inflammation

Stephen J. Skehan, MD[1]; Jessica F. White, MD[1]; John W. Evans, MD[1]; David R. Parry-Jones, MSc[1]; Chandra K. Solanki, BSc[1]; James R. Ballinger, PhD[1]; Edwin R. Chilvers, PhD[2]; and A. Michael Peters, MD[1]

[1]*Department of Nuclear Medicine, Addenbrooke's Hospital, Cambridge, United Kingdom; and*
[2]*Department of Medicine, Addenbrooke's and Papworth Hospitals, Cambridge, United Kingdom*

^{99m}Tc-Sulesomab, the Fab fragment of anti–NCA-90, is used as an in vivo granulocyte labeling agent for imaging inflammation. It is not clear to what extent it targets cells that have already migrated into the interstitial space of an inflammatory lesion as opposed to circulating cells. The contribution to signal of radioprotein diffusion in the setting of increased vascular permeability is also poorly documented. **Methods:** We compared the local kinetics of ^{99m}Tc-sulesomab and ^{99m}Tc-labeled human serum albumin (HSA), which have similar molecular sizes, in 7 patients with orthopedic infection proven by clearly positive ^{111}In-leukocyte scintigraphy. ^{99m}Tc-Sulesomab and ^{99m}Tc-HSA were administered in sequence separated by an interval of 2–6 d. Images were obtained 1, 3, 4, and 6 h after injection, and multiple venous blood samples were obtained for blood clearance measurement. Patlak–Rutland (P–R) analysis was performed to measure lesion and control tissue protein clearance. Target-to-background tissue (T/Bkg) ratios were calculated for each radioprotein and compared with the T/Bkg ratio for ^{111}In-leukocytes. ^{99m}Tc-Sulesomab binding to granulocytes was measured in vitro and ex vivo and to primed and activated granulocytes in vitro. **Results:** After intravenous injection, <5% of the circulating radioactivity was cell bound with both radioproteins so that the P–R curves could therefore be assumed to represent extravascular uptake of free protein. The blood clearance (mean ± SD) of sulesomab was 23.4 ± 11.7 mL/min, ~5 times greater than that of HSA, for which it was 4.8 ± 3.1 mL/min. Likewise, clearance into the lesion of sulesomab was consistently higher than that of HSA, on average about 3 times as high. Nevertheless, the T/Bkg ratios for sulesomab and HSA were similar, except at 6 h when that of HSA (2.14 ± 0.6) was higher than that of sulesomab (1.93 ± 0.5; $P \sim 0.01$). Both values were considerably less than the T/Bkg ratio on the ^{111}In-leukocyte images, which, at 22 h, was 12.3 ± 5.3. Moderate clearance of sulesomab, but not HSA, was seen in the control tissue. Granulocytes bound significantly more ^{99m}Tc-sulesomab in vitro when primed or activated. **Conclusion:** (a) Sulesomab does not localize in inflammation as a result of binding to circulating granulocytes; (b) sulesomab is cleared into inflammation nonspecifically via increased vascular permeability; nevertheless, it may be cleared after local binding to primed granulocytes or bind to activated, migrated extravascular granulocytes; and (c) HSA produces a similar or higher T/Bkg ratio than sulesomab because sulesomab is cleared into normal tissues and because image positivity in inflammation is significantly dependent on local blood-pool expansion.

Key Words: infection; antibodies, monoclonal; radiopharmaceuticals; granulocytes; tissue distribution

J Nucl Med 2003; 44:11–18

A radiolabeled murine monoclonal antibody fragment, ^{99m}Tc-sulesomab (LeukoScan; Immunomedics Europe, Hillegom, The Netherlands), is used increasingly for imaging inflammation (*1–6*). The suggested mechanism of action of this tracer is binding to NCA-90 surface antigen on granulocytes, theoretically allowing in vivo labeling of granulocytes after intravenous injection. The antibody fragment is radiolabeled with ^{99m}Tc in a simple 5-min procedure, avoiding the time-consuming and potentially dangerous technique of in vitro leukocyte labeling, which, insofar as it is the technique against which new inflammation-targeting agents are generally compared, would be regarded as the gold standard for imaging acute inflammation. Although some of the injected tracer may bind to circulating granulocytes, other mechanisms of localization in areas of inflammation are also possible. It is known, for instance, that capillary permeability increases in inflamed tissues, allowing increased diffusion of proteins into the interstitial space (*7*). It has also been suggested that the antibody may preferentially bind to extravascular granulocytes that have migrated and become activated (*8*).

The purpose of this study was to examine these mechanisms, especially the relative contribution of nonspecific capillary permeability, to the ^{99m}Tc-sulesomab signal. Its uptake kinetics were therefore compared with those of a simple protein of similar size, ^{99m}Tc-labeled human serum albumin (HSA), in inflamed and normal tissues. Tracer binding to and elution from granulocytes was also assessed, both with respect to circulating granulocytes in vivo and harvested granulocytes in vitro. In the latter instance, uptakes of sulesomab and ^{18}F-FDG were compared between control, primed, and fully activated granulocytes.

Received Mar. 25, 2002; revision accepted Jul. 26, 2002.
For correspondence or reprints contact: A. Michael Peters, MD, Department of Nuclear Medicine, Box 170, Addenbrooke's Hospital, Hills Rd., Cambridge, CB2 2QQ, U.K.
E-mail: michael.peters@addenbrookes.nhs.uk

MATERIALS AND METHODS

In Vitro Studies of Leukocyte Binding

Granulocytes were isolated from healthy volunteer blood using discontinuous plasma/Percoll (Amersham Pharmacia Biotech, Uppsala, Sweden) gradients, washed, and resuspended in 90 μL of platelet-poor plasma (1.5×10^6 per condition) and subjected to priming and activation stimuli as described by Kitchen et al. (*9*). Granulocyte purity was assessed by light microscopy and viability was assessed by trypan blue exclusion. Cells were incubated at 37°C for 30 min in a thermomixer with either phosphate-buffered saline (PBS) or tumor necrosis factor-α (TNF-α) at a priming concentration of 200 U/mL. After 30 min, formyl-Met-Leu-Phe (fMLP; final concentration, 100 nmol/L) or PBS was added for 5 min to induce, in the case of fMLP, full activation. ^{99m}Tc-Sulesomab or ^{99m}Tc-HSA was then added (1.8–8.9 kBq ^{99m}Tc on 3–75 μg protein in 100 μL saline) followed by incubation for a further 30 min. Each condition was performed in triplicate. Reactions were terminated by the addition of 1 mL ice-cold PBS, and the cells were centrifuged at 14,000*g* for 5 min. Aliquots of 100 μL of the supernatant were removed for counting, and the remaining supernatant was aspirated carefully, so as not to disturb the granulocyte cell pellet. The cell pellet was washed once in PBS and spun down again before aspiration. Radioactive counts of the supernatant and the pellet were then obtained in a γ-well counter. The fraction of added radioactivity bound to the cell pellet was calculated.

For the ^{18}F-FDG studies, cells were isolated and prepared in the same way and resuspended in PBS. Priming and activating conditions were the same, but ^{18}F-FDG was added after TNF-α and immediately before fMLP—that is, before full activation of the cells. After a further 35 min, ^{18}F-FDG uptake was stopped by the addition of 100 nmol/L iodoacetic acid. Cells were then centrifuged and washed in the same manner as above before comparing radioactivity counts in the supernatants and the pellets. Each condition was performed in triplicate with 1.5×10^6 cells per condition used.

Studies of in vitro binding of ^{99m}Tc-sulesomab to leukocytes were also performed by adding ^{99m}Tc-sulesomab to anticoagulated whole blood obtained from healthy volunteers. After 1 h of incubation, the leukocytes were harvested as described above, and the amount of ^{99m}Tc activity associated with the leukocytes was measured. The cells were then resuspended in fresh plasma and the stability of the label in plasma was determined at room temperature over 2 h. A second aliquot of ^{99m}Tc-sulesomab was added directly to leukocytes that had been harvested from blood from the same volunteer. The labeling efficiency after 15 min at room temperature and the stability of the label were determined as above.

Clinical Studies

Patients. During the study period of 14 mo, all patients with peripheral orthopedic infection, as evidenced by a clearly positive ^{111}In-leukocyte scan, were invited to participate in the study. Patients with infections of the axial skeleton were excluded to avoid confounding physiologic visceral and bone marrow activity. Patients with equivocal leukocyte scans, those unable to give fully informed consent, and those who had participated in a research project involving ionizing radiation in the previous 12 mo were excluded. The local research ethics committee approved the study and all patients gave their written, informed consent.

Binding and Elution Studies. Studies of in vivo leukocyte binding of both ^{99m}Tc-sulesomab and ^{99m}Tc-HSA was performed on 2 of the 7 patients. After samples of whole blood had been taken for counting, the residue was centrifuged to allow measurement of cell-associated activity. The buffy coat was transferred to a fresh tube, the red blood cells were lysed with water, and the remaining activity in the pellet was assumed to be bound to leukocytes.

Imaging. All patients were imaged with both ^{99m}Tc-sulesomab and ^{99m}Tc-HSA on separate days at least 2 d apart and at least 5 d after the ^{111}In-leukocyte scan. The order of the examinations was randomized to minimize any effect due to treatment or changes in the patient's clinical condition between the 2 examinations. Sulesomab was labeled with ^{99m}Tc in accordance with the manufacturer's instructions; radiochemical purity was >95%. ^{99m}Tc-HSA was prepared by electrolytic labeling of commercially obtained HSA (Zenalb 20; Bio Products Laboratory, Elstree, Herts, U.K.) (*10*). The specific activity of ^{99m}Tc-HSA was 28–39 MBq/mg, and the radiochemical purity remained >97% throughout the experiment as determined by thin-layer chromatography. Both radioproteins were given at a dose of 500 MBq. An identical protocol for imaging and blood sampling was followed for both tracers. Intravenous cannulas were placed in both arms, one for administering the tracer and the other for taking blood samples. After taking a baseline sample, the radioprotein was injected and blood samples were taken at 5, 30, 60, 120, 180, 240, and 360 min after injection. Imaging of the inflamed area and the adjacent normal tissue was performed at 60, 180, 240, and 360 min after injection. The view chosen was based on the optimal view from the preceding ^{111}In-leukocyte study. Static images were acquired for 5 min using a high-resolution collimator and a 256×256 matrix.

Data Analysis. Regions of interest (ROIs) were drawn closely around the area of inflammation and larger ROIs over the control areas. Decay-corrected counts per pixel were calculated for each ROI at each time point. Target-to-background (T/Bkg) ratios were calculated at each time point. Saponified whole-blood samples were counted in a well counter along with a standard prepared from the same vial as the injected dose. After correction for decay, dead time, and, in 1 case, minor downscatter from the preceding ^{111}In-leukocyte study, blood counts were expressed as a percentage of the injected dose per liter. Biexponential curves were fitted to the blood time–activity curves for calculation of blood radioprotein clearance. Patlak–Rutland (P–R) graphical analysis (*11*) was used to measure local tissue clearance of each radioprotein. In the event of unidirectional uptake from blood, the gradient of the P–R plot is proportional to tissue clearance and the zero time intercept is proportional to local tissue blood volume. A nonlinear plot implies bidirectional transfer, with instantaneous gradient reflecting net transfer. Because not all plots were linear, no attempt was made to quantify tissue clearance. Instead, a second-order polynomial was fitted to quantify the local blood volumes given by the radioproteins. These have units of mL/pixel × k (where k is a constant equal to the ratio of counting efficiencies of the well counter and the gamma camera) and clearly should be identical between the 2 radioproteins. In addition, target-to-blood ratios were compared between sulesomab and HSA at specific times after injection.

Statistics. Comparisons between radiotracers were based on the paired Student *t* test. Correlations between radiotracers were based on linear regression analysis. $P < 0.05$ was considered significant. Unless otherwise stated, values are presented as mean ± SD.

RESULTS

In Vitro Studies of Leukocyte Binding

When ^{99m}Tc-sulesomab was added to donor whole blood and incubated for 60 min at room temperature, 2.2% of the radioactivity was bound to leukocytes. After resuspension in saline for 120 min, 70% of the radioactivity remained on the cells. When ^{99m}Tc-sulesomab was incubated with isolated leukocytes for 15 min, 4.5% binding was obtained, although only 43% of this remained after 120 min in saline.

For the in vitro assays, granulocyte purity and viability were routinely >95% (with <0.5% monocytes) and >99.5%, respectively. Sulesomab bound preferentially to primed and activated granulocytes in these assays. After correction for nonspecific binding to the microcentrifuge tube, there was 5.39% ± 1.54% binding of sulesomab to fully activated granulocytes compared with 5.53% ± 3.43% to cells primed with TNF-α and 1.5% ± 1.25% to quiescent granulocytes incubated with plasma alone ($P < 0.05$ compared with full activation). ^{99m}Tc-HSA binding to control and primed cells was undetectable and to fully activated granulocytes was only 0.86% ± 1.04% (Fig. 1).

^{18}F-FDG uptake by primed and activated granulocytes mirrored this pattern with more avid uptake of glucose seen in the primed and activated states (Fig. 1). Granulocytes coincubated with TNF-α accumulated 45.8% ± 6.8% of total radioactivity, whereas fully activated cells accumulated 52.9% ± 9.9% of total activity compared with 14.8% ± 1.51% in quiescent granulocytes also incubated with ^{18}F-FDG for 35 min (Fig. 1; $P < 0.005$ compared with primed and fully activated cells).

Clinical Studies

Patients. Seven patients (5 males; age, 36–72 y; mean age, 58 y), of 10 patients who were approached, volunteered for the study. Two had infections in the elbow, 1 in a total knee replacement, 1 in the humerus, 2 in the ankle, and 1 in the foot. In 1 case, symptoms of infection had been present for 2 wk before diagnosis with leukocyte scintigraphy, whereas in the other 6 cases, the patients had been symptomatic for >3 mo. The time interval between the ^{111}In-leukocyte scan and the first of the 2 study examinations ranged from 6 to 16 d (mean, 8.6 d), and the time interval between the 2 study examinations ranged from 2 to 6 d (mean, 3.4 d). ^{99m}Tc-Sulesomab was administered first in 4 cases.

Blood Clearance. Measurements of cell-associated radioactivity in the circulation were performed in 2 patients. For ^{99m}Tc-sulesomab, 1.56% ± 0.81% and 3.82% ± 2.89% of the circulating radioactivity was associated with cells in the 2 patients, respectively, averaged over 6 or 7 time points. The corresponding values for ^{99m}Tc-HSA were 0.73% ± 1.40% and 3.32% ± 2.89%. Of this cell-associated radioactivity, 2.0%–20.8% for ^{99m}Tc-sulesomab and 1.9%–5.1% for ^{99m}Tc-HSA was associated with leukocytes.

Blood clearances of ^{99m}Tc-sulesomab and ^{99m}Tc-HSA were 23.4 ± 11.7 and 4.8 ± 3.1 mL/min, respectively ($P <$

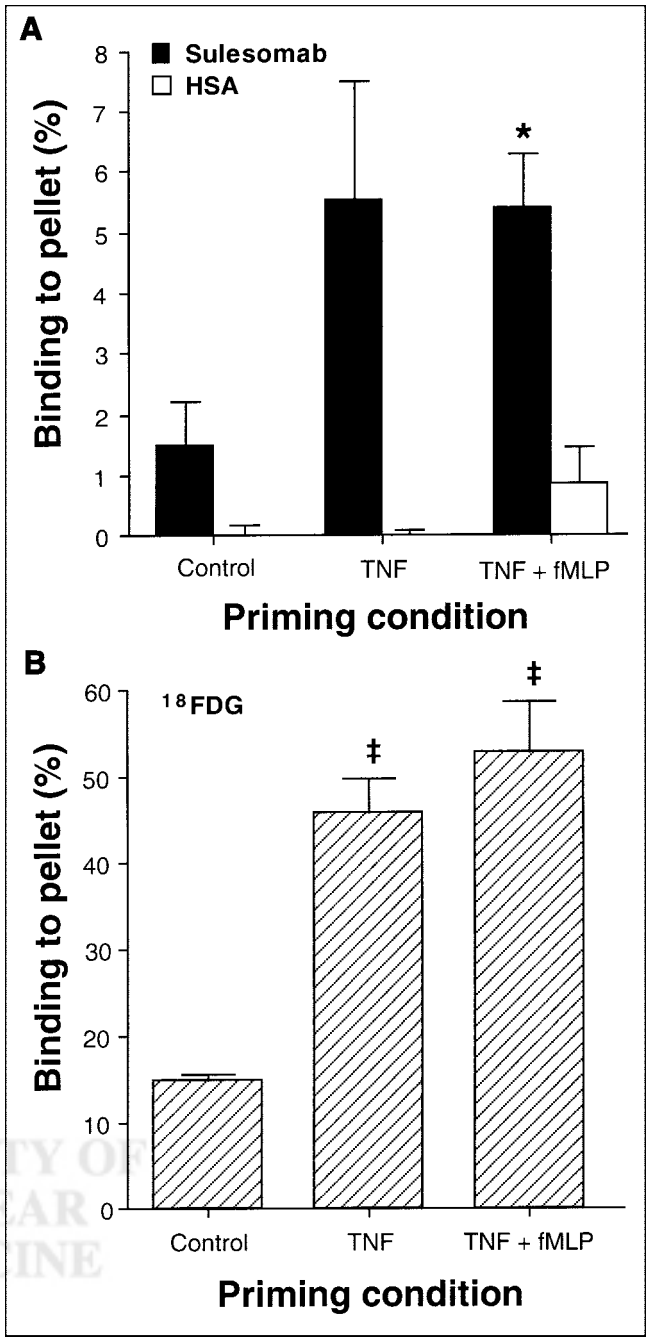

FIGURE 1. Binding of ^{99m}Tc-sulesomab and ^{99m}Tc-HSA (A) and ^{18}F-FDG (B) to quiescent control, TNF-α-primed, and TNF-α-primed, fMLP fully activated granulocytes, shown as percentage uptake of available tracer by cells (mean ± SE). ^{99m}Tc-Sulesomab or ^{99m}Tc-HSA was added to suspension of granulocytes after they had been incubated with TNF-α (or PBS) for 30 min and exposed to fMLP (or PBS) for additional 5 min. ^{18}F-FDG was added to suspension of granulocytes after they had been incubated with TNF-α (or PBS) for 30 min and immediately before addition of fMLP (or PBS). Data are corrected for nonspecific binding ($n = 3$ for each column). *Significant difference compared with control cells at $P < 0.05$. ‡Significant difference compared with control cells at $P < 0.005$.

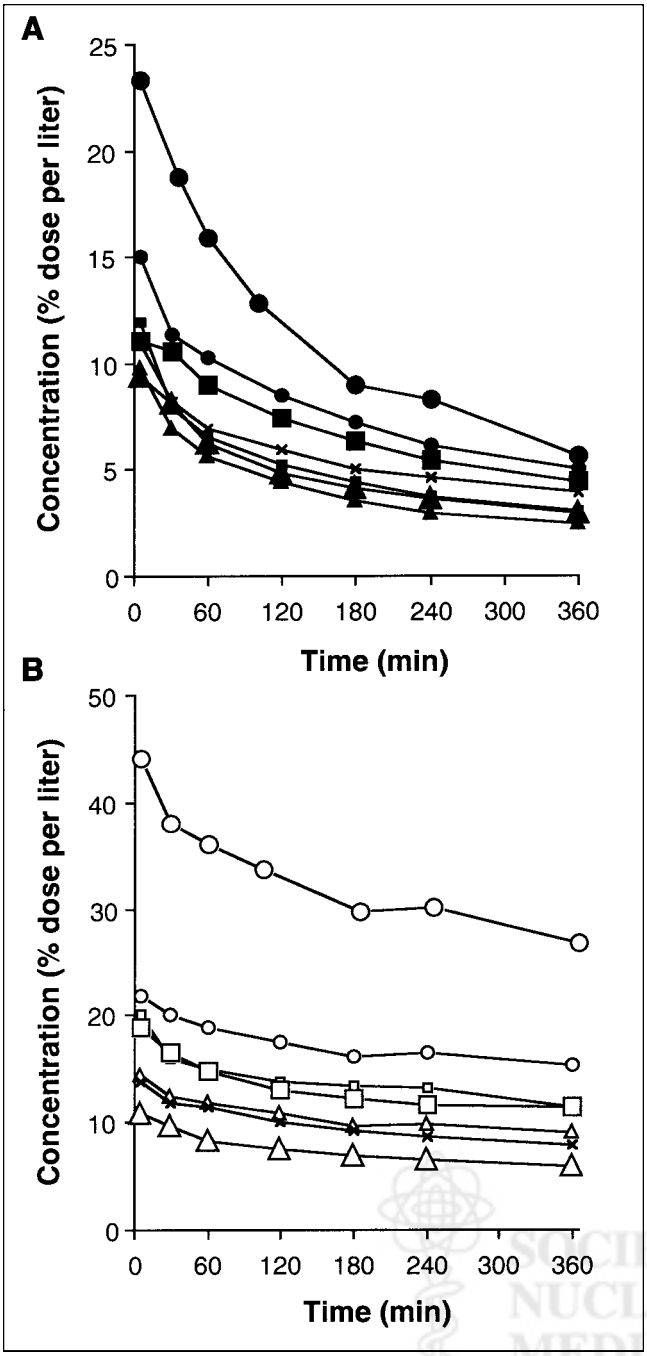

FIGURE 2. Blood clearances of ^{99m}Tc-sulesomab (A) and ^{99m}Tc-HSA (B) in each individual subject. Symbol shapes (filled and open symbols) here and in Figure 4 correspond to 1 individual patient.

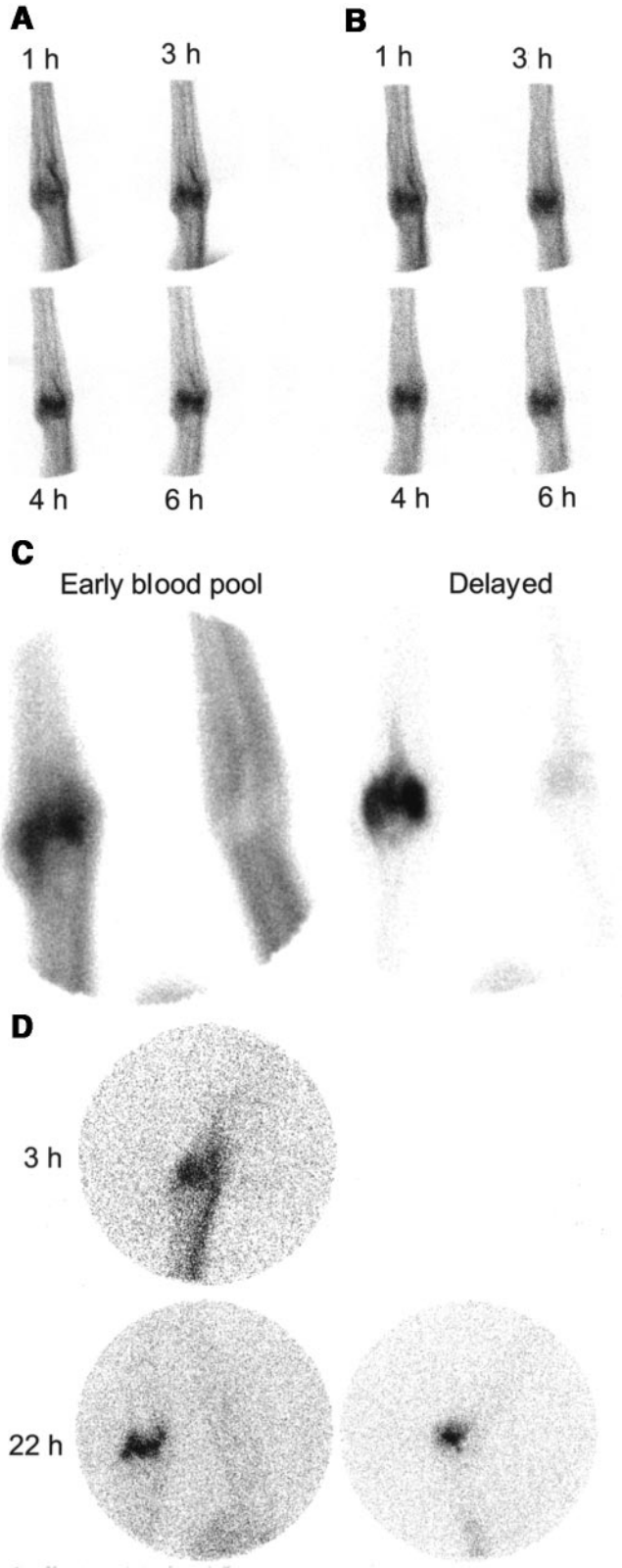

FIGURE 3. Radioprotein images of patient with septic arthritis of elbow acquired 1, 3, 4, and 6 h after injection: (A) ^{99m}Tc-HSA; (B) ^{99m}Tc-sulesomab. ^{99m}Tc-Methylene diphosphonate images (C) and 22-h ^{111}In-leukocyte images (D) are shown for comparison.

0.001) (Fig. 2). There was no significant correlation between them.

Imaging and P–R Analysis. Focal uptake was seen with both radioproteins at the site of inflammation in all cases (Fig. 3). Visual inspection of the images showed broadly similar appearances with both radioproteins, although greater blood-pool activity was visible on the later images with ^{99m}Tc-HSA than with ^{99m}Tc-sulesomab, reflecting its

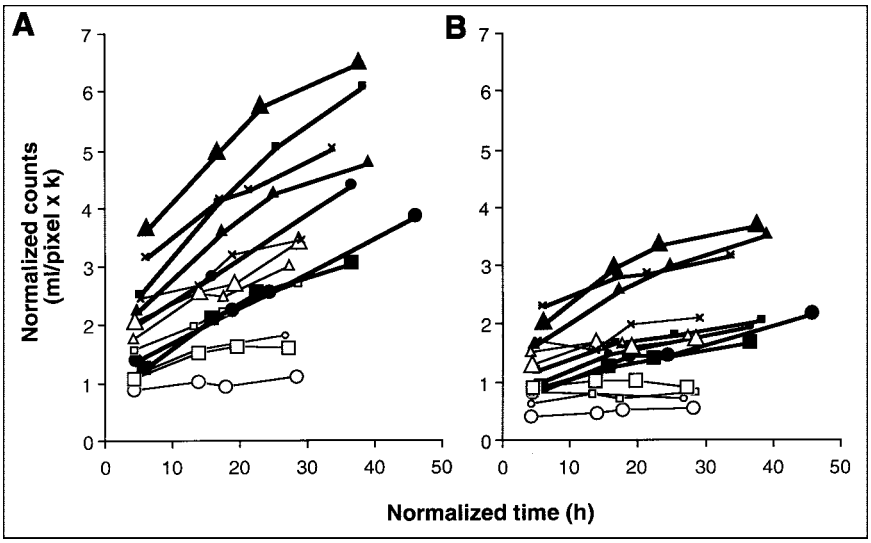

FIGURE 4. P–R plots illustrate tissue clearance of ^{99m}Tc-sulesomab (filled symbols, bold lines) and ^{99m}Tc-HSA (open symbols, fine lines) in all 7 patients. Symbol shapes correspond to same patients as in Figure 2. (A) Site of infection. (B) Control tissue.

slower blood clearance. P–R graphical analysis showed that the local net clearance of ^{99m}Tc-sulesomab into areas of infection was clearly greater than that of ^{99m}Tc-HSA in all 7 patients (Fig. 4A). In comparison with 6 of 7 HSA P–R plots, only 2 of 7 P–R sulesomab plots were linear, the remainder being clearly convex upward, precluding measurement of the P–R gradient and, hence, of clearance. However, in all patients and at all 4 imaging time points, the target-to-blood ratio (the ordinate of the P–R plot or normalized counts) was higher for sulesomab than that for HSA, with mean values shown in Table 1. The local blood volume in the lesion, which corresponds to the zero-time intercept of the P–R plot, was slightly but significantly higher for sulesomab with a mean value of 1.74 ± 0.71 mL/pixel × k, compared with 1.34 ± 0.54 mL/pixel × k for HSA ($P < 0.02$). P–R analysis showed that clearance of sulesomab into normal background tissues was also greater than that of HSA in all 7 patients. There was essentially no detectable ^{99m}Tc-HSA clearance into normal tissues (Fig. 4B). There was no difference in local blood volume of control tissue, with respective mean values of 1.09 ± 0.48 mL/pixel × k for sulesomab and 0.97 ± 0.48 mL/pixel × k for HSA. Local blood volume was significantly higher in the lesion compared with the control tissue for both sulesomab and HSA.

T/Bkg Ratios. The mean T/Bkg ratios at 6 h after injection for sulesomab and HSA were 1.93 ± 0.52 and 2.14 ± 0.6, respectively ($P < 0.01$) (Table 2). No significant differences in the mean T/Bkg ratios were seen at the other time points. The T/Bkg ratios for ^{111}In-labeled leukocytes at both 3 h (5.6 ± 4.5) and 22 h (12.3 ± 5.3) were higher than for both sulesomab and HSA in all 7 patients ($P < 0.01$). There was a strong correlation between sulesomab and HSA with respect to the 6-h T/Bkg ratio ($r = 0.97$; $P < 0.01$) (Fig. 5), with less obvious correlation at earlier time points. In contrast, there was no significant correlation between the ^{111}In-labeled leukocyte T/Bkg ratio and that of either radioprotein (Fig. 5).

DISCUSSION

Sulesomab is directed against the nonspecific cross-reacting antigen of molecular weight 90 kDa (NCA-90), which is expressed on the surface of granulocytes and is also known as CD66c (*12*). The highly homologous NCA family of glycoproteins is related immunologically and structurally to carcinoembryonic antigen and is found on the epithelium of the lung and colon, macrophages, and colonic adenocarcinoma, in addition to granulocytes (*12*).

TABLE 1
Target-to-Blood Ratios

Tracer	1 h	3 h	4 h	6 h
Sulesomab	2.34 ± 0.87	3.44 ± 1.07	4.09 ± 1.31	4.82 ± 1.2
HSA	1.57 ± 0.57	1.99 ± 0.64	2.2 ± 0.8	2.45 ± 0.93
P (sulesomab vs. HSA)	<0.01	<0.01	<0.01	<0.01

See Figure 4.

TABLE 2
T/Bkg Ratios

Patient no.	^{111}In-Leukocytes		HSA				Sulesomab			
	3 h	22 h	1 h	3 h	4 h	6 h	1 h	3 h	4 h	6 h
1	5.8	16.4	1.81	2		2.51	2.13	1.91		2.25
2	14.5	15.1	2.15	2.15	1.83	2.06	1.69	1.56	1.76	1.75
3	7.7	13	1.91	2.48	3.09	3.31	2.08	2.45	2.76	2.95
4	4.3	18.5	1.19	1.52	1.59	1.78	1.42	1.66	1.8	1.82
5	1.5	2.8	1.17	1.51	1.5	1.67	1.37	1.39	1.43	1.36
6	2.9	11.6	1.61	1.52	1.68	1.97	1.8	1.66	1.71	1.76
7	2.3	8.7	1.44	1.73	1.61	1.65	1.37	1.48	1.51	1.6
Mean	5.6	12.3	1.61	1.84	1.88	2.14*	1.69	1.73	1.83	1.93
SD	4.5	5.3	0.37	0.38	0.6	0.6	0.33	0.36	0.48	0.52

* $P \sim 0.01$ vs. sulesomab (paired Student *t* test).

^{99m}Tc-Sulesomab has been licensed for several years for use in patients with suspected infection. Clinical studies have demonstrated promising diagnostic efficacy of sulesomab in the detection of musculoskeletal, gastrointestinal, and cardiac infections (*1–6*). Some reports have claimed it to be as effective as or superior to ^{111}In-labeled leukocytes (*4,5*). Sulesomab is thought to target inflammation as a result of binding in vivo to NCA-90 surface antigen of circulating granulocytes. Expression of NCA-90 is increased over baseline levels in activated granulocytes (*13*), so it is reasonable to expect that sulesomab would show greater binding to activated granulocytes than to quiescent granulocytes and that it may therefore target granulocytes that are about to migrate or have already migrated and become activated, as suggested (*8*). However, the contribution to the target signal of nonspecific transendothelial diffusion through the abnormally permeable microvasculature of inflamed tissue has received little attention. This study attempted to address this issue by comparing local tissue clearance of ^{99m}Tc-sulesomab with that of ^{99m}Tc-HSA, a reference molecule of similar molecular size to that of sulesomab. We also directly measured sulesomab binding to granulocytes, both in vitro and ex vivo.

It is clear from this study that sulesomab shows very little binding to circulating granulocytes, with the ex vivo cell labeling studies demonstrating <5% cell binding of the administered sulesomab activity. This finding is consistent with whole-body imaging, which shows only a limited resemblance to the normal whole-body image of labeled granulocytes in that splenic activity in particular is not especially prominent in sulesomab whole-body images (*14*). A similar minimal level of ex vivo cell binding was found with ^{99m}Tc-HSA, which has no specific affinity for granulocytes, suggesting minimal nonspecific association of small circulating proteins with leukocytes. It is unlikely that this small amount of cell-associated activity is sufficient to produce a detectable signal at the site of infection.

The plasma and local clearance studies showed a consistent pattern in all 7 patients. Tissue clearance of sulesomab into areas of infection was greater than that of HSA. In the absence of significant binding to circulating granulocytes, it is not clear why this should be. A component of sulesomab clearance into an inflammatory lesion will be due to nonspecific capillary permeability to small proteins (*7*) and reflected by the HSA clearance rate. The molecular sizes of the molecules are similar, so, bearing in mind that molecular diffusibility is broadly proportional to the cube root of molecular weight (*15*), differences in microvascular permeability do not adequately explain the difference in lesion clearance rates. Nonspecific clearance would be expected to be bidirectional, but it is possible that sulesomab clearance could be predominantly unidirectional if there was binding to extravascular activated granulocytes, resulting in an apparently higher rate of clearance. Nevertheless, sulesomab clearance was higher than that of HSA in control tissue. Because there was no active bone marrow in the region of these inflammatory lesions, other mechanisms must be considered, one of which might be cross-reaction to endothelial cells constitutively expressing CD66a (*16,17*).

Preferential binding of sulesomab to activated granulocytes in vitro is confirmed in this study. Binding of sulesomab and uptake of ^{18}F-FDG by granulocytes is increased by both priming and full activation. However, the level of sulesomab binding, even to fully activated cells, is low at no more than about 5%. We would suggest from these in vitro studies that, in vivo, sulesomab does not localize in inflammation as a result of binding to circulating granulocytes alone but, like ^{18}F-FDG, may target inflammation as a result of uptake by granulocytes that are functionally different from circulating granulocytes. Both sulesomab and ^{18}F-FDG are taken up more avidly by primed and activated cells. Sulesomab binds to the upregulated CD66c moiety, whereas ^{18}F-FDG is taken up by metabolically active cells as a surrogate of glucose. The 2 different experimental protocols were designed to demonstrate this, with ^{18}F-FDG added before full activation of cells, and sulesomab added after maximal expression of CD66c on the cell surface. The

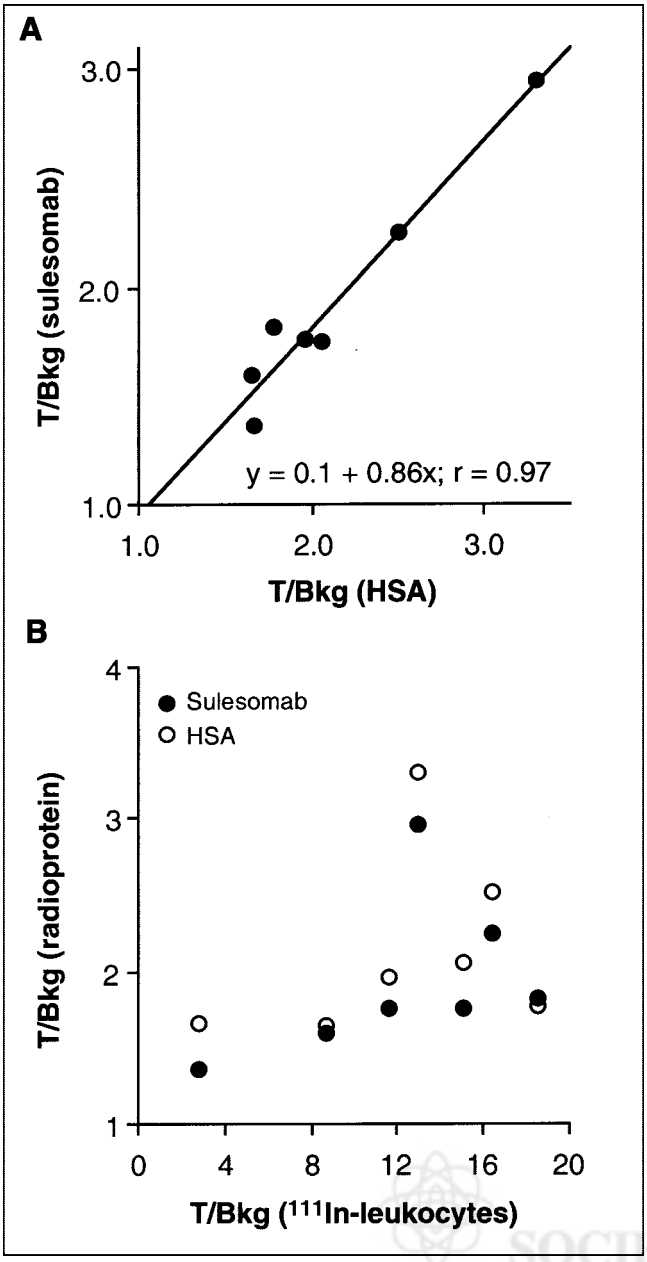

FIGURE 5. Correlation between T/Bkg ratios of ^{99m}Tc-sulesomab and ^{99m}Tc-HSA (6 h) (A) and between T/Bkg ratios of ^{111}In-leukocytes (22 h) and ^{99m}Tc-sulesomab and ^{99m}Tc-HSA (6 h) (B).

similarity in their targeting kinetics is reflected by the common features displayed in Figure 1.

Sulesomab is a fraction antibody targeted against CD66c (the NCA-90 epitope) that is upregulated in primed and activated granulocytes (*13*). CD66c may also be expressed on endothelium, which would explain faster clearance compared with radiolabeled HSA into normal tissues in vivo. In contrast, ^{18}F-FDG was taken up avidly by both primed and activated neutrophils in comparison with that of quiescent cells. This would suggest that both priming and full activation of granulocytes in vitro is an energy-dependent process and that granulocytes use exogenous glucose rather than depend entirely on endogenous stores.

Translation of in vitro binding data to the in vivo situation, however, is hazardous because the radioprotein has less access to granulocytes, which in turn must compete with avid sulesomab binding to bone marrow antigens. The latter is largely responsible for the faster plasma clearance of sulesomab compared with that of HSA. An interesting possibility is that sulesomab may bind preferentially to primed or activated intravascular granulocytes marginating in the lesion, before being carried across the endothelium by granulocyte migration. This would explain both the higher clearance rate and the apparently higher lesion blood volume (zero-time P–R intercept) found for sulesomab in comparison with HSA. Nevertheless, if sulesomab did bind to local granulocytes, a closer correlation between T/Bkg ratios for sulesomab and ^{111}In-leukocytes might have been expected; instead, the sulesomab T/Bkg ratio correlated better with the HSA T/Bkg ratio, suggesting vascular permeability to be the predominant factor.

In addition to a higher tissue clearance, plasma clearance of sulesomab was also more rapid than that of HSA. Both of these factors should promote a higher T/Bkg ratio for sulesomab, but the ratio was similar for the 2 radioproteins at 1, 3, and 4 h after injection and greater for HSA than for sulesomab at 6 h. The higher lesion clearance of sulesomab is therefore presumably offset by its higher clearance in control tissue. Fast blood clearance is generally considered an advantage in terms of optimizing the T/Bkg ratio because high levels of blood activity contribute to the background signal. The slower plasma clearance of HSA would be expected to confer a higher blood-pool activity for this protein. However, blood-pool activity also contributes to the target signal in areas of inflammation as a result of expansion of the local blood pool, and this would also offset any advantage to sulesomab of a more rapid plasma clearance. The importance of a blood-pool signal has been emphasized recently by Rennen et al. (*18*), who found no dependence of radiopeptide or radioprotein uptake into sepsis on molecular weight but a high dependence on the circulatory residence time.

CONCLUSION

The mechanism of action of ^{99m}Tc-sulesomab remains unclear, although it is not related to intravascular binding of the tracer to circulating granulocytes. Nevertheless, sulesomab has a higher clearance into inflammatory lesions than that of ^{99m}Tc-HSA, possibly as a result of local binding to activated granulocytes. It also has a faster blood clearance, which should reduce its background signal. Nevertheless, sulesomab and HSA gave similar T/Bkg ratios in areas of inflammation. This finding is explained by the important contribution of blood-pool activity, which increases the target signal for HSA, and by clearance of sulesomab into normal tissues, which increases the background signal for

sulesomab. Even allowing for bias of patient selection, however, neither radioprotein gave T/Bkg ratios that approached those given by ^{111}In-leukocytes.

ACKNOWLEDGMENTS

The authors are grateful to Dr. Karen Cadwallader for technical advice relating to granulocyte isolation, to The Wolfson Brain Imaging Centre for supplying ^{18}F-FDG, and to GlaxoSmithKline for financial support. This work was supported in part by Immunomedics Europe, who donated kits for the preparation of ^{99m}Tc-sulesomab, and in part by the Medical Research Council and a Sackler fellowship.

REFERENCES

1. Barron B, Hanna C, Passalaqua AM, Lamki L, Wegener WA, Goldenberg DM. Rapid diagnostic imaging of acute, nonclassic appendicitis by leukoscintigraphy with sulesomab, a technetium 99m-labeled antigranulocyte antibody Fab′ fragment: LeukoScan Appendicitis Clinical Trial Group. *Surgery.* 1999;125:288–296.
2. Becker W, Bair J, Behr T, et al. Detection of soft-tissue infections and osteomyelitis using a technetium-99m-labeled anti-granulocyte monoclonal antibody fragment. *J Nucl Med.* 1994;35:1436–1443.
3. Becker W, Palestro CJ, Winship J, et al. Rapid imaging of infections with a monoclonal antibody fragment (LeukoScan). *Clin Orthop.* 1996;329:263–272.
4. Harwood SJ, Valdivia S, Hung GL, Quenzer RW. Use of sulesomab, a radiolabeled antibody fragment, to detect osteomyelitis in diabetic patients with foot ulcers by leukoscintigraphy. *Clin Infect Dis.* 1999;28:1200–1205.
5. Hakki S, Harwood SJ, Morrissey MA, Camblin JG, Laven DL, Webster WBJ. Comparative study of monoclonal antibody scan in diagnosing orthopaedic infection. *Clin Orthop.* 1997;335:275–285.
6. Gratz S, Raddatz D, Hagenah G, Behr T, Behe M, Becker W. ^{99m}Tc-Labelled antigranulocyte monoclonal antibody FAB′ fragments versus echocardiography in the diagnosis of subacute infective endocarditis. *Int J Cardiol.* 2000;75:75–84.
7. Arfors K-E, Rutili G, Svensjo E. Microvascular transport of macromolecules in normal and inflammatory conditions. *Acta Physiol Scand Suppl.* 1979;463:93–103.
8. Becker W, Repp R, Hansen HJ, Goldenberg DM, Wolf F. Binding characteristics and kinetics of a new Tc-99m-antigranulocyte Fab fragment (Leukoscan™) [abstract]. *J Nucl Med.* 1995;36(suppl):208P.
9. Kitchen E, Rossi AG, Condliffe AM, Haslett C, Chilvers ER. Demonstration of reversible priming of human neutrophils using platelet-activating factor. *Blood.* 1996;88:4330–4337.
10. Millar AM, Hannan WJ, Sapru RP, Muir AL. An evaluation of six kits of technetium-99m human serum albumin injection for cardiac blood pool imaging. *Eur J Nucl Med.* 1979;4:91–94.
11. Peters AM. Graphical analysis of dynamic quantitative data. *Nucl Med Commun.* 1994;15:669–672.
12. Stocks SC, Ruchaud-Sparagano MH, Kerr MA, Grunert F, Haslett C, Dransfield I. CD66: role in the regulation of neutrophil effector function. *Eur J Immunol.* 1996;26:2924–2932.
13. Klein ML, McGhee SA, Baranian J, Stevens L, Hefta SA. Role of nonspecific cross-reacting antigen, a CD66 cluster antigen, in activation of human granulocytes. *Infect Immun.* 1996;64:4574–4579.
14. Saverymuttu SH, Peters AM, Keshavarzian A, Reavy HJ, Lavender JP. The kinetics of 111-indium distribution following injection of 111-indium labelled autologous granulocytes in man. *Br J Haematol.* 1985;61:675–685.
15. Crone C, Levitt DJ. Capillary permeability to small solutes. In: Renkin EM, Michel CC, eds. *The Cardiovascular System.* Vol. IV, part 1. Bethesda, MD: American Physiological Society; 1984:411–466.
16. Yamanaka T, Kuroki M, Matsuo Y, Matsuoka Y. Analysis of heterophilic cell adhesion mediated by CD66b and CD66c using their soluble recombinant proteins. *Biochem Biophys Res Commun.* 1996;219:842–847.
17. Prall F, Nollau P, Neumaier M, et al. CD66a (BGP), an adhesion molecule of the carcinoembryonic antigen family, is expressed in epithelium, endothelium, and myeloid cells in a wide range of normal human tissues. *J Histochem Cytochem.* 1996;44:35–41.
18. Rennen HJJM, Makarewicz J, Oyen WJG, Laverman P, Corstens FHM, Boerman OC. The effect of molecular weight on nonspecific accumulation of ^{99m}Tc-labeled proteins in inflammatory foci. *Nucl Med Biol.* 2001;28:401–408.